Dimensional metrology of bipolar fuel cell plates using laser spot triangulation probes

Dimensional metrology of bipolar fuel cell plates using laser spot triangulation probes

Bala Muralikrishnan, Wei Ren, Dennis Everett, Eric Stanfield and Ted Doiron

Mechanical Metrology Division, National Institute of Standards and Technology, Gaithersburg, MD 20899, USA

E-mail: balam@nist.gov

Abstract

As in any engineering component, manufacturing a bipolar fuel cell plate for a polymer electrolyte membrane (PEM) hydrogen fuel cell power stack to within its stated design tolerances is critical in achieving the intended function. In a bipolar fuel cell plate, the dimensional features of interest include channel width, channel height, channel parallelism, side wall taper, straightness of the bottom or side walls, plate parallelism, etc. Such measurements can be performed on coordinate measuring machines (CMMs) with micro-probes that can access the narrow channels. While CMM measurements provide high accuracy (less than 1 μm), they are often very slow (taking several hours to measure a single plate) and unsuitable for the manufacturing environment. In this context, we describe a system for rapid dimensional measurement of bipolar fuel cell plates using two laser spot triangulation probes that can achieve comparable accuracies to those of a touch probe CMM, while offering manufacturers the possibility for 100% part inspection. We discuss the design of the system, present our approach to calibrating system parameters, present validation data, compare bipolar fuel cell plate measurement results with those obtained using a Mitutoyo UMAP (see footnote 1) fiber probe CMM, and finally describe the uncertainty in channel height and width measurements.

Keywords: dimensional metrology, fuel cell, laser triangulation

(Some figures in this article are in colour only in the electronic version)

1. Introduction

Bipolar plates used in polymer electrolyte membrane (PEM) hydrogen fuel cell stacks are manufactured from a variety of materials and manufacturing processes, and have varied designs (plate thickness, material, coating, number of channels and their layout, etc are all design variables) [1, 2]. In order to achieve the performance specifications, it is critical that the plate be manufactured to stated tolerances [3–6]. Dimensional metrology of bipolar fuel cell plates is a critical aspect in the design, manufacture and eventual use of these plates in a PEM hydrogen fuel cell stack. The features of interest in these plates include channel width and height, parallelism of the channels, plate parallelism, side wall taper, straightness of the bottom or side walls, etc.

High accuracy dimensional measurements on bipolar plates can be made using micro-probes on coordinate measuring machines (CMMs) [7, 8]; the high aspect ratios of the channels preclude the use of traditional macro-scale CMM probes. These contact-based measurements provide micrometer-level accuracies, but are exceedingly slow. A measurement of the entire plate for all the features of interest mentioned above could easily take several hours.

We have developed a laser triangulation-based non-contact probing system that can perform rapid measurements, yet achieve accuracies comparable to those of a CMM. We
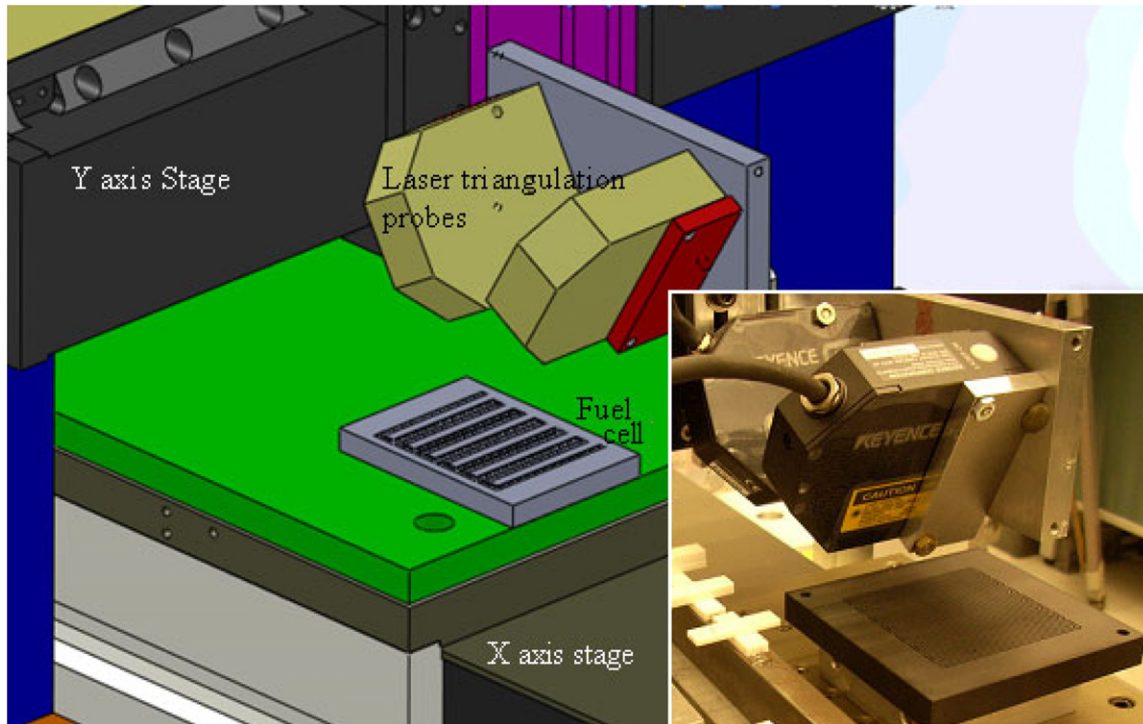
Figure 1. The fuel cell metrology station showing two laser triangulation probes, each tilted in opposing directions to obtain side wall information.

describe the system in the next section, describe the probe's scale and linearity errors in section 3, detail the procedure used to calibrate system parameters in section 4, present validation data in section 5, discuss measurement results on fuel cell plates in section 6, present an uncertainty budget in section 7, and summarize key results in section 8.

This paper primarily focuses on width and height measurements of fuel cell plates because we have comparison data on these features from a Mitutoyo UMAP[1] contact probing system. Further, validation data using gauge blocks can also be used to substantiate our claims on uncertainty for channel width and height measurements. We should note however that the profile data obtained using our non-contact probing system may be used to compute other features such as side wall taper (if any), plate parallelism, straightness of the channel bottom, etc.

2. Dual laser probe fuel cell metrology station system description

Laser spot triangulation probes offer both the required range (a few millimeters) and the necessary resolution (sub-micrometer) to perform accurate dimensional measurements on fuel cell plates. A laser spot triangulation probe in conjunction with an *XY* stage provides a convenient way of performing dimensional measurements on different artifacts.

---

[1] Commercial equipment and materials are identified in order to adequately specify certain procedures. In no case does such identification imply recommendation or endorsement by the National Institute of Standards and Technology, nor does it imply that the materials or equipment identified are necessarily the best available for the purpose.

If only a single probe is used, and this probe is set up to look straight down on a fuel cell plate as it is scanned across, the finite spot size of the probe limits the ability to detect the transition from horizontal to vertical surface near the channel's side wall and therefore limits the accuracy with which channel width can be detected. Further, a single probe looking straight down provides no information on the side walls of the channel, such as its taper and form. We therefore utilize two probes that are tilted in opposing directions so that each probe can capture data on one side wall and some part of the bottom of the channel. This dual-probe scheme is shown in figure 1. Our system utilizes two Keyence[1] LK-G32 laser spot triangulation probes, an Aerotech[1] ALS 50060 stage for the *X* axis and an Aerotech[1] PRO 115 stage for the *Y* axis. We do not take special care in aligning the part on the table. A visual alignment to within a couple of degrees is sufficient for channel width and height calculations as our uncertainty budget shows (see section 7).

Six system parameters have to be determined for our dual-probe system by prior calibration before the system can be used for the measurement of bipolar fuel cell plates. These are (refer to figure 2) as follows.

- θ_1: tilt of the first probe in the *XZ* plane. This is nominally set to $-25°$.
- θ_2: tilt of the second probe in the *XZ* plane. This is nominally set to $25°$.
- w: horizontal offset measured as the distance between the probes' zero readings along the *X* axis.
- v: vertical offset measured as the distance between the probes' zero readings along the *Z* axis.
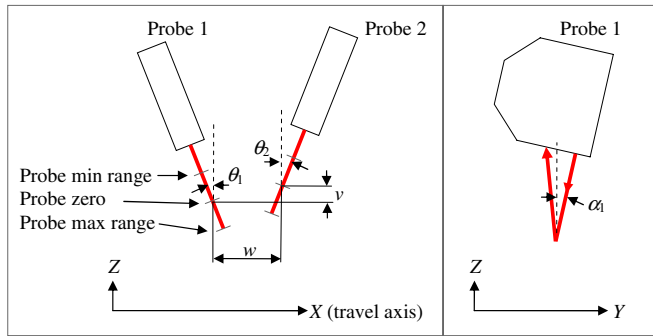
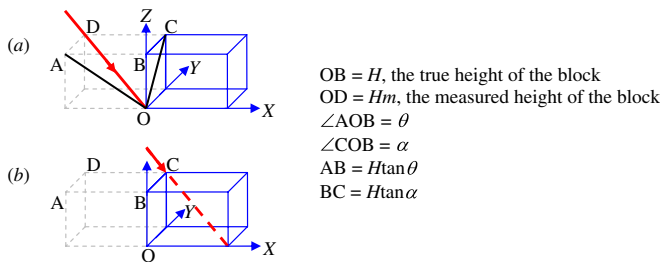**Figure 2.** Fuel cell metrology station system parameters.

OB = H, the true height of the block
OD = Hm, the measured height of the block
$\angle AOB = \theta$
$\angle COB = \alpha$
AB = $H\tan\theta$
BC = $H\tan\alpha$

Figure 3. The laser is incident at an angle θ in the XZ plane and at an angle α in the YZ plane. (*a*) A gauge block (shown in solid line) is placed along the X axis so that the laser is incident at point O. (*b*) The probe is translated along the positive X direction. The laser is now incident at point C instead of point B (because of a non-zero misalignment angle α, the laser strikes at different Y positions for different heights).

- α_1: misalignment of the first probe in the YZ plane. This is nominally zero.
- α_2: misalignment of the second probe in the YZ plane. This is nominally zero (not shown in figure 2).

Assuming that the system parameters are completely known, the measured data which are in a non-orthogonal frame (because the probe is inclined at an angle θ in the XZ plane and may also be misaligned by angle α in the YZ plane) have to be corrected to an orthogonal frame before any features of interest can be evaluated.

The geometry of the measurement is shown in figure 3. Suppose that the laser makes an angle θ in the XZ plane (we have dropped the subscript for θ and α because the description is valid for both probes) and an angle α in the YZ plane (α is a misalignment angle; its nominal value is zero). Let the probe be used to scan along the vertical face of a gauge block with the intent of measuring the X and Z coordinates of points O and B.

In figure 3(*a*), a gauge block of height H (OB in figure 3) is placed along the X axis so that the laser strikes the point O. The probe's measurements are along the DO direction. Let the probe reading at this position be zero. Then, let the probe be translated along the positive X direction (while the probe is stationary in our setup, we assume that the probe is translated here to simplify the discussion) so that the laser just strikes the top surface of the block, see figure 3(*b*). Because there is a non-zero misalignment angle α, the laser strikes the top surface at a slightly displaced Y position (point C instead

of point B in figure 3(*b*)). From the geometry in the figure, the displacement Hm measured by the probe as it travels from O to C (equal to OD in the figure) is given by

$$Hm = H(\sqrt{1 + \tan^2\theta + \tan^2\alpha}). \tag{1}$$

If point O is assumed to be the origin for the measurement, the measured X and Z coordinates of point C (Xm, Hm) in the non-orthogonal frame is given by ($H\tan\theta$, $H(\sqrt{1 + \tan^2\theta + \tan^2\alpha})$). Our objective is to determine the X and Z coordinates of point B (Xc, Zc) in an orthogonal frame of reference; its coordinates can be determined from the measured coordinates of C through the following correction:

$$
\begin{aligned}
Xc &= Xm - H\tan\theta \\
&= Xm - Hm\tan\theta/(\sqrt{1 + \tan^2\theta + \tan^2\alpha}), \\
Zc &= Hm/(\sqrt{1 + \tan^2\theta + \tan^2\alpha}).
\end{aligned}
\tag{2}
$$

It should be noted that the Y coordinate of point C is different from that of B, the difference being equal to $H\tan\alpha$. This simply means that the probe measures a point at a location different from the desired location along Y. This is not of major consequence if α is small. We account for this in the uncertainty budget.

We next describe our method to determine the parameters θ and α and the uncertainty in those parameters. But first, we discuss scale (and linearity) errors in the laser triangulation probes because errors from the probes are expected to be one of the dominant sources of uncertainty in our measurements.

3. Assessing scale errors in the probes

Laser triangulation probes suffer from numerous sources of error, many of which are coupled with the surface characteristics of the part under inspection. Garces *et al* [9] provide an excellent review of these error sources. We describe an uncertainty budget for our measurements in section 7 where we describe efforts to address the issues described in [9]. One of the primary contributors to uncertainty in our system is the scale and linearity errors (the scale error is simply a linear term; we define linearity errors as the residual from the scale error) in the probing system. We discuss linearity tests here.

The scale (and linearity) errors in the two laser triangulation probes were determined by comparison against a laser interferometer. For this experiment, the laser triangulation probes were made to measure the surface of a ceramic gauge block; the blocks were oriented so that the probe's laser was incident normal to the part. The results of the comparison are shown in figure 4. The alignment of the triangulation probes with the laser interferometer was verified to be within 0.2°; this angle is extremely small and has a negligible impact on the scale error. The results show that one of the probes has a negative scale error of $-0.21\,\mu\text{m}\,\text{mm}^{-1}$ while the other probe has a positive scale error of $0.49\,\mu\text{m}\,\text{mm}^{-1}$. Although small, we compensate the measured data for the above mentioned scale errors. Further, the linearity error (the residual error after correcting for the slope) is within $\pm 2\,\mu\text{m}$, which is smaller than the manufacturer's specification of $\pm 5\,\mu\text{m}$, at least for the ceramic gauge blocks.
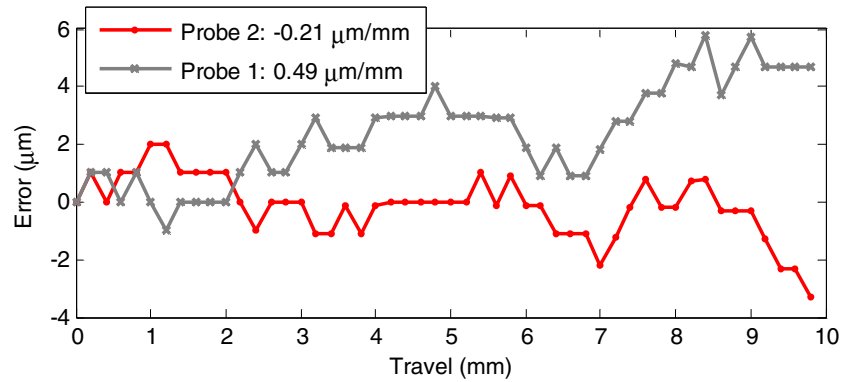
Figure 4. Scale errors in the laser triangulation probes.

Because the probes are tilted in our setup, the laser from the probe is not normal to either the top or side wall surfaces during the measurement of a fuel cell plate. In order to determine the dependence of angle of incidence on linearity errors, two linearity experiments were performed—one with the surface normal oriented at a $25°$ angle relative to the laser from the probe and the other with the surface normal oriented at a $65°$ angle relative to the laser from the probe. These angles were selected because they correspond to the angles of incidence relative to the top and side wall surfaces of a fuel cell during measurement. The linearity errors varied from ± 3 μm to ± 7 μm for the surfaces angled at $25°$ and $65°$, respectively. We have noticed that the linearity errors can vary not only with angular orientation but also with the surface characteristics of the part under inspection. In our uncertainty evaluations, we therefore use the manufacturer's specification for linearity errors of ± 5 μm for horizontal surfaces, and our experimentally determined ± 7 μm linearity errors for side wall examination, when the full range of the probe is used. When smaller probe ranges are used for the measurement, we attenuate the bounds as appropriate.

4. Procedure to estimate the tilt angle θ and the misalignment angle α

4.1. Using calibrated height blocks

A relatively simple procedure to determine the tilt angle θ would involve the use of one calibrated height block of height H. Assuming that $\alpha = 0$ and also assuming that the scale error s (in units of millimeter per millimeter) in the probe is zero (we assume that the linearity errors are zero as well; non-zero linearity is treated as a source of uncertainty), the measured height Hm is simply given by

$$Hm = H(\sqrt{1 + \tan^2 \theta}) = H/\cos \theta. \quad (3)$$

Therefore, an estimate for θ, given by θ', can be obtained fairly easily as

$$\theta' = \cos^{-1}(H/Hm). \quad (4)$$

When $\alpha \neq 0$ and/or $s \neq 0$, the measured height Hm is given by

$$Hm = H(\sqrt{1 + \tan^2 \theta + \tan^2 \alpha + s}). \quad (5)$$

The scale error s can be independently measured and the measured probe readings can be compensated, as we showed in section 3. Therefore we do not include s in further discussions here.

When $\alpha \neq 0$, we can then obtain an estimate θ' using equation (4), but such an estimate will be in error. Some simple computations (using equations (4) and (5)) can be performed to determine the magnitude of this error. Let the nominal value of θ be $25°$ and let the misalignment angle α be $1°$. Then, the resulting estimate for the tilt angle θ' is $25.015°$, or the error in θ' is $0.015°$.

4.2. Uncertainty in the tilt angle θ from the height block method

A real measurement is not only influenced by a possible non-zero misalignment angle α, it is further corrupted by the probe's repeatability and linearity errors, errors in the motion (due to the stage), etc. A Monte Carlo simulation (MCS) considering

- probe linearity errors of ± 5 μm (all values within this bound are considered equally likely and therefore we model this error using a uniform distribution),
- misalignment angle α modeled using a normal distribution with a standard deviation of $0.3°$ (we estimate that our alignment is approximately within the $\pm 1°$ interval, which we regard as three standard deviations of a normal distribution), and
- stage Z straightness modeled as a uniform distribution with ± 3 μm bound

reveals a standard uncertainty of $0.075°$ in θ' using the height block method.

Note that the probe repeatability is approximately ± 2 μm. However, we average numerous data points on both the top surface of the plate and the bottom surface of the channel to determine the height. Assuming that 1000 data points are available (sampled at 1 μm spacing), the uncertainty due to repeatability is less than 0.1 μm. Probe linearity error, on the other hand, cannot be averaged out, as this is a systematic error in the probe's ranging ability.

We will discuss the implications of this uncertainty in the tilt angle θ on fuel cell plate measurements in a later section.

But first, we point out that this technique of using height blocks does not provide a way of separating the effects of misalignment angle α and tilt angle θ on height measurements. Next, we present an alternate approach to obtaining an estimate for the tilt angle θ that will substantially reduce the errors for the same assumptions on the misalignment angle α, while also allowing the separation of the effects of misalignment angle α and tilt angle θ when the scale error is known.

4.3. Estimating the tilt angle θ from profile measurements on vertical surfaces

The tilt angle θ can be determined from vertical profile measurements as we show in this section. We refer again to figure 3. Let the probe read a value of zero at O, see figure 3(*a*). Assume that the probe is then translated along the positive X direction so that it strikes the upper edge of the gauge block at point C, as shown in figure 3(*b*). The magnitude of this translation (AB in figure 3(*a*)) is a known quantity determined from the X axis encoder readings. The change in probe readings as the probe travels from O to C is given by Hm, and is also a known quantity. From the geometry shown in figure 3, we note that

$$AB = H \tan \theta,$$
$$DO = Hm = H(\sqrt{1 + \tan^2 \theta + \tan^2 \alpha}). \tag{6}$$

For the special case when $\alpha = 0$, the direction of incidence of the laser beam DO is coincident with its projection in the XZ plane, AO. The probe therefore travels from O to B instead of to C. In this case, we can accurately determine the tilt angle θ from the two measured quantities AB and AO (=DO) using the relation

$$\theta = \sin^{-1}(AB/AO). \tag{7}$$

When $\alpha \neq 0$, we can determine an estimate for the tilt angle θ' using the approximation AO $\approx$ DO:

$$\theta' = \sin^{-1}(AB/DO). \tag{8}$$

We calculate the error in θ' to be $-0.003°$ for the assumptions stated in the preceding section ($\theta = 25°$, $\alpha = 1°$). This error is substantially smaller than the $0.015°$ error obtained using the height block method.

A further interesting aspect of this approach is that this technique allows the separation of the effects of tilt angle θ and misalignment angle α and thereby allows the estimation of both θ and α accurately. We will next demonstrate how this may be done through measurements on calibrated height blocks.

Because we do not initially know the value of the misalignment angle α and therefore assume that it is zero, we can obtain an estimate for the Z coordinate of point B, given by Zc', as

$$Zc' = Hm \cos \theta'. \tag{9}$$

From equations (6) and (8), we can relate the estimate θ' to the theoretical values of θ and α to obtain

$$Zc' = Hm\sqrt{(1 + \tan^2 \alpha)}/\sqrt{1 + \tan^2 \theta + \tan^2 \alpha}$$
$$= H/\cos \alpha. \tag{10}$$

The corrected X coordinate for point B (Xc') can then be obtained as

$$Xc' = Xm - Zc \tan \theta', \tag{11}$$

where Xm is the measured X coordinate of point B (encoder reading). Substituting equations (6), (8) and (9) into equation (11) we obtain

$$Xc' = Xm - Hm \sin \theta' = Xm - H \tan \theta. \tag{12}$$

4.3.1. Implications of correcting measured data with the estimate θ'.
Equation (12) shows that the corrected X coordinate of point B, Xc, is in fact the true coordinate of point B. There is no error after the correction process. This is because if O is considered as the origin, the measured coordinate of point B, given by Xm, is equal to the amount of translation along the X axis. This is given by AB in figure 3 and is equal to $H \tan \theta$. The corrected X coordinate of point B, Xc', is therefore zero as expected.

The Z coordinate of point B (the estimate Zc') does suffer from an error. That error is inversely proportional to $\cos \alpha$ (see equation (10)). Therefore an estimate for the misalignment angle α can be determined by measuring a calibrated height block. The estimate for α can then be used to revise the value of θ'. If the real value of the misalignment angle α is $1°$, the measured height of a calibrated gauge block will be longer as shown in equation (10). We therefore use equation (10) to estimate the new value for the misalignment angle α, which turns out to be exactly $1°$. Applying this value for the misalignment angle, we can now refine the estimate for θ' to obtain the theoretical value of $25°$. Therefore, in theory, we can estimate the values of α and θ accurately using the vertical profile method. Real measurements suffer from noise and other sources of uncertainty; we discuss the uncertainty in the estimation of the angles α and θ next.

4.4. Uncertainty in the tilt angle θ from vertical profile measurements

The largest contributor to the uncertainty in the tilt angle θ is the error motion of the Y axis stage. We have experimentally determined the standard uncertainty due to repeatability in θ to be $0.02°$ due to variations in the Y position, possibly due to roll motions of the Y stage. All other sources of uncertainty are significantly smaller in comparison so that we can consider $0.02°$ to be the standard uncertainty in θ.

It should be noted that should lower uncertainties be required, an *in situ* calibration of the tilt angle can be performed at the exact Y location where the part profile is obtained. Such a scheme is not required for fuel cell plate measurements as our uncertainty calculations in section 7 show. If such an *in situ* calibration scheme were to be adopted, the uncertainty in θ will be much smaller than the $0.02°$ repeatability term mentioned earlier. We list the influence factors below for the sake of completeness.

- *Incorrect estimation of the misalignment angle α.* We model the error in α using a normal distribution of zero mean and $0.3°$ standard deviation.

- *Probe linearity errors*. The measured probe reading *Hm* suffers from a linearity error; we mentioned in section 3 that this error has a ±7 μm bound. We assume that any value within this bound is equally likely and therefore model this error using a uniform distribution.
- *X axis encoder errors*. The manufacturer's specification for the *X* axis encoder errors are ±1 μm. Again, we assume that any value in this bound is equally likely and use a uniform distribution to model this error.
- *Pitch motion of the stage*. The stage has a 17 arc-seconds pitch specification. It is unlikely that there will be large pitch variations over a short travel range. Therefore we do not consider local pitch variations as a source of error. The more likely effect of the pitch error is to produce a tilt in the vertical surface. For purposes of uncertainty estimation, we assume that any pitch value within a ±17 arc-seconds bound is possible, and further a setup tilt of ±0.003° is possible (this value is experimentally determined). It should be noted that pitch errors can potentially be mapped at the *Y* location where profiles are being measured; we have not done so because the contribution due to this term is not substantial.

Assuming that a data point is acquired every 1 μm along the *X* axis and a gauge block of height 5 mm is measured with the probe nominally at 25°, MCS reveals a standard uncertainty in the tilt angle θ of 0.003° for the case where *in situ* calibration is performed at every *Y* position where the profile is acquired.

4.5. Uncertainty in the misalignment angle α from vertical profile measurements

After determining an estimate for the tilt angle θ (which is nominally 25°), the misalignment angle α can be determined from a measurement of a calibrated height. Assuming that a block with a height of 5 mm is used for the measurement, and further assuming that the probe linearity error is ±5 μm, the standard uncertainty in θ is 0.02°, and the *Z* straightness of the stage is within ±3 μm, a MCS produces a standard uncertainty in α of 0.078°.

4.5.1. The need to estimate the misalignment angle α.
The misalignment angle α is not a dominant contributor to the uncertainty in the measurements for our setup where α is nominally zero (see section 7). However, in some cases where the part surfaces are highly reflective, the probe is required to have a larger angle α [10]. In such situations, the angle α does have a comparable role as the tilt angle θ in the uncertainty in measurements. It is therefore necessary to be able to separate the effects of θ and α, and therefore the vertical profile measurement is a better approach than the calibrated height block method.

4.6. Procedure to estimate offsets and their uncertainties

The vertical offset can be determined by measuring a horizontal profile on a high quality surface (such a gauge block which has been aligned parallel to the machine's table) using both probes. The difference in average readings of the two

Table 1. Width errors on thin Mitutoyo blocks.

Nominal (mm)	Measured value[a] (mm)	Errors (μm)
2.54	2.5402	0.2
3.175	3.1744	−0.6
5.08	5.0791	−0.9
6.35	6.3501	0.1
7.62	7.6199	−0.1

[a] The expanded uncertainties in our width measurements are 6 μm ($k = 2$); see section 7 for an explanation. We note that the nominal values may be different from the calibrated values by at most 0.1 μm. This is not of much consequence to our measurements as our claimed uncertainty is larger by an order of magnitude. This comment applies to subsequent tables 2 and 3 as well.

probes is the vertical offset. The vertical offset does not impact width and height measurements but will play a role in tying the data from the probes into a common frame. The standard uncertainty in the vertical offset is less than 0.1 μm because of the considerable number of averaging that takes place in its computation.

The horizontal offset can be determined by measuring a gauge block of known width. One probe measures one vertical face of the block, while the other probe measures the opposing face. The difference between the measured width (which is the difference between the measured *X* coordinates of the two faces of the block) and the true width is the horizontal offset. The standard uncertainty in the horizontal probe offset is 2.1 μm (we describe the calculation of this uncertainty in section 7).

5. System validation

We describe experiments using ceramic gauge blocks to assess the performance of the system. Ceramic gauge blocks, such as fuel cell plates, have matte surfaces which produce diffuse reflection. The misalignment angle α is nominally zero for such surfaces. Steel blocks, on the other hand, have polished surfaces that produce specular reflection; the probes are required to have a larger angle α in such cases. The experiments were primarily performed to determine the width and height measurement capability of the system. They also very clearly demonstrate one of the weaknesses of laser triangulation probes, namely their sensitivity to material properties.

5.1. Width measurements on gauge blocks of similar material properties

Several ceramic gauge blocks were carefully aligned on the table so that the calibrated dimension of the blocks was parallel to the travel axis of the stage (the *X* axis). The dual-probe system was calibrated according to the method described in section 2. The widths of the blocks were then measured; the results are shown in table 1. It can be seen that the errors are less than ±1 μm; this suggests that we can in fact measure widths with an uncertainty that is potentially comparable to that obtainable on a CMM.

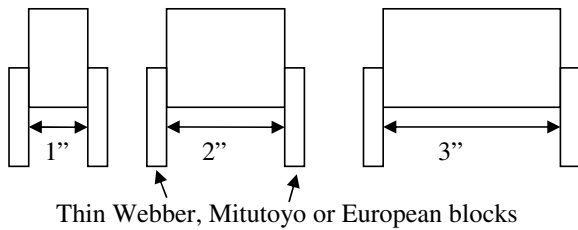**Figure 5.** Width measurements across the gap created using thin blocks

Table 2. Width errors in micrometers.[a]

	1 inch	2 inch	3 inch
European	0	0.4	1.1
Mitutoyo	−4.5	−4.6	−5.1
Webber	−7.1	−5.6	−6.1

[a] The expanded uncertainties in our width measurements are 6 μm ($k = 2$); see section 7 for an explanation.

5.2. Width measurements on gauge blocks to illustrate the influence of material properties

It is well known that laser triangulation probes are very sensitive to the material properties of the components under measurement. The following experiment clearly reveals the extent of this problem. Three ceramic blocks, a 1-inch, 2-inch and 3-inch, were considered for the experiment. Instead of directly measuring the width of the blocks across their side walls, we wrung two thin ceramic blocks to their gauging surfaces and measured the internal distance between the two thin blocks as shown in figure 5. The purpose of wringing the thin blocks is to present the same surface for all three gauge blocks; therefore, we removed the two thin blocks from the 1-inch block after the measurement and subsequently wrung the same blocks to the 2-inch and 3-inch block for the measurement.

Subsequently, we chose two other sets of two thin blocks and repeated the measurements on the 1-inch, 2-inch and 3-inch blocks. Although all three sets of thin blocks appear to be visually similar, the widths obtained using the different blocks varied considerably, as shown in table 2. We refer to the thin blocks as European (British Standards blocks), Mitutoyo and Webber[1]. The results are shown in table 2. The offset between the probes was calibrated using the 1-inch gauge block measured with the thin European blocks. Therefore, that entry (in the first row and first column) has a zero error.

The results indicate that the errors in the measurement of the 1-inch, 2-inch and 3-inch gauge blocks are small (less than ±1 μm) if the probe offset calibration is performed using blocks of similar material. For example, the errors when using the Mitutoyo blocks are −4.5 μm, −4.6 μm and −5.1 μm for the 1-inch, 2-inch and 3-inch blocks respectively when using the European 1-inch block as the master. If a Mitutoyo 1-inch block were instead used as the master, the errors for the 2-inch and 3-inch blocks would only be −0.1 μm and −0.6 μm respectively. That is, the range of the errors is small across any row in the table. But the range of errors is large across a column indicating that changing the material seen by the probe can have a large influence on the measured length. For

Table 3. Height errors on Webber blocks.

Nominal (mm)	Measured value[a] (mm)	Error (μm)
2.794	2.7939	−0.1
3.81	3.8109	0.9
4.826	4.8251	−0.9

[a] The expanded uncertainties in our height measurements are 3.8 μm ($k = 2$); see section 7 for an explanation.

example, the first column shows that if the same 1-inch gauge block is measured with three different thin gauge blocks of slightly different material properties, we can potentially see large errors, up to 7 μm, between measurements.

This experiment clearly demonstrates the sensitivity of laser triangulation probes to material properties. In order to avoid large errors in width measurements of fuel cell plates, it is necessary to calibrate the probe offset using a master made of identical material to the part.

5.3. Height measurements on gauge blocks

Three gauge blocks of known height were wrung to three other gauge blocks to form three pairs of cross-blocks. The cross-block pairs were placed on the table and profiles were obtained across the blocks. Surface data from top of the upper block and top of the lower block were used to determine the heights of the blocks. The errors in the heights are shown in table 3. They are also less than ±1 μm suggesting that potentially high accuracy measurements are feasible using the dual-probe laser triangulation system.

6. Graphite bipolar fuel cell plate measurement results

Two graphite bipolar fuel cell plates with nominally vertical side walls were measured using both a Mitutoyo UMAP touch-probe CMM and the dual-probe laser triangulation system. The data obtained using the UMAP system are considered the reference data for the triangulation probe measurements. Each plate contained three parallel channels, each making 15 turns, for a total of 45 rows. The UMAP system was used to obtain the channel width and height of each of those 45 rows for plate 1 and 21 rows for plate 2 along the centerline of the plates. The laser triangulation probes were then used to measure profiles along the same centerline, from which we calculated channel width and height. The laser triangulation probe measurements were performed at 30 mm s^{-1} with a sampling interval of 1 μm.

For the UMAP measurements, the channel height was defined as the distance between the bottom of the channel (data acquired from the central 0.25 mm of the plate) and a least-squares line fit to the data acquired from the top surface, while assuming that the plate was fixtured on a vacuum chuck to remove its bend. The width was defined as the distance between two opposing points at a depth of 0.3 mm from the top surface. As in the case of height measurements, the part was fixtured on a vacuum chuck to remove its bend, and a least-squares best fit line was established by probing the top surface.
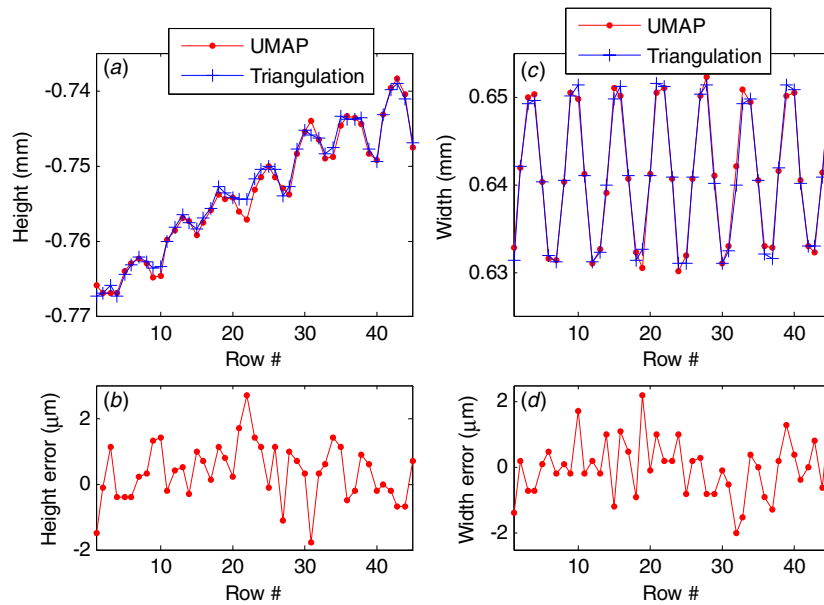
Figure 6. Plate 1: (*a*) measured height of each row using both the UMAP and the dual-probe laser triangulation systems; (*b*) height error for each row; (*c*) measured width of each row using both the UMAP and the dual-probe laser triangulation systems; (*d*) width error for each row (note that the width errors shown here do not include any potential bias in the measurement because the probe offset w was determined from the measurement of this plate). The expanded uncertainties in our height and width measurements are 3.8 μm ($k = 2$) and 6 μm ($k = 2$) respectively; see section 7 for an explanation.
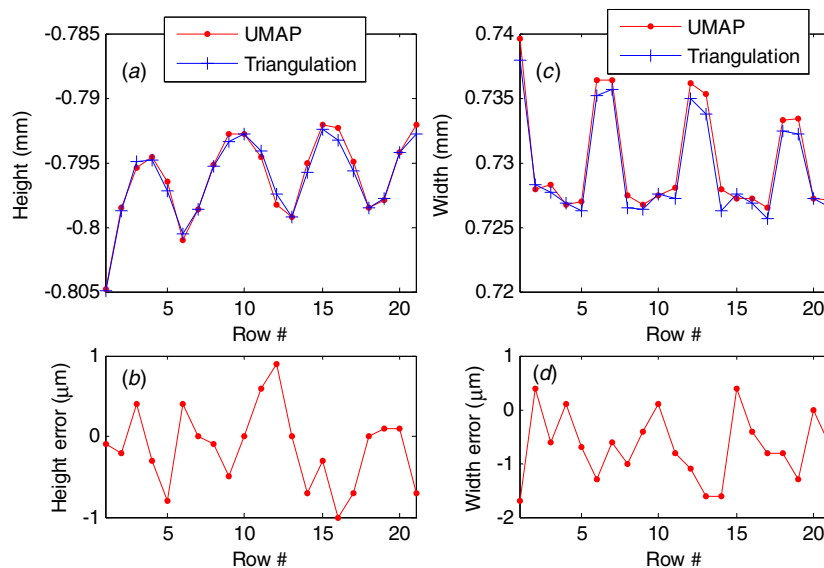

Figure 7. Plate 2: (*a*) measured height of each row using both the UMAP and the dual-probe laser triangulation systems; (*b*) height error for each row; (*c*) measured width of each row using both the UMAP and the dual-probe laser triangulation systems; (*d*) width error for each row (because the probe offset was determined from a measurement of plate 1, the width errors for plate #2 do reflect any bias in the measurement, although none is apparent in the results). The expanded uncertainties in our height and width measurements are 3.8 μm ($k = 2$) and 6 μm ($k = 2$) respectively; see section 7 for an explanation.

As mentioned earlier, laser triangulation probes are extremely sensitive to material properties and therefore, we used plate 1 to determine the horizontal offset w for the probing system (the average width of all rows determined from the UMAP system was subtracted from the average width of all rows determined using the dual-probe laser system to determine the offset). We then applied this offset for plate 2 to determine channel widths. The results are shown in figures 6 and 7.

Figures 6(*b*) and 7(*b*) show that the height measurements with our non-contact probing system are within ±2 μm of the UMAP values. This is within our uncertainty; we estimate an expanded uncertainty of 3.8 μm ($k = 2$) for height measurements with our non-contact probe, as we demonstrate in the next section, while the expanded uncertainty for height measurements for the UMAP system is 0.5 μm ($k = 2$).

Figure 7(*d*) shows that the width measurements are also within ±2 μm of the UMAP values when the probe offset is calibrated with a master of similar material (in this case,

we use width values obtained from the UMAP on plate 1 as the master). Again, this is within our uncertainty; we estimate an expanded uncertainty of 6 μm ($k = 2$) for width measurements with our non-contact probe, as we demonstrate in the next section, while the expanded uncertainty for width measurements for the UMAP system is 1.7 μm ($k = 2$).

7. Uncertainty in width and height measurements

The error sources in a laser triangulation probe have been extensively studied before [9]. The laser triangulation probes are sensitive to bright–dark transitions, to secondary reflections near the intersection of two surfaces (such as near the intersection between a side wall and the bottom of a channel), to material properties that cause volumetric scattering, part roughness, etc.

The error sources detailed in [9] impact measurements made on materials of different colors, parts with large form (for example, spherical or conical surfaces), etc. The measurements made on fuel cell plates, however, are not affected by many of the issues described in that report. We do however notice the problem of secondary reflections near the bottom of the channel where some small portion of the data has to be discarded.

One potential source of large errors is related to the sensitivity of the probe to material properties. This may be related to the problem of volumetric scattering mentioned in [9]. In section 5.2 we showed, via experiment, the influence of material property on the measured channel width. Because the system requires a calibration of the probe offset w, and this probe offset is material dependent, it becomes critical to calibrate the probe using a master made out of a material that is identical to the part under inspection. While this is a limitation of this measurement technology, it is a tradeoff to obtaining high accuracy in the measurements.

The following uncertainty calculations are made under the assumption that the channel height $H = 1$ mm and that the side walls are nominally vertical. A summary is tabulated in table 4; a description follows.

7.1. Height measurements

7.1.1. Uncertainty in the estimation of the tilt angle θ. The measured height Hm is corrected for the tilt angle θ to determine the true height H as $H = Hm \cos\theta$. The uncertainty in θ was estimated earlier (section 4.4) to be 0.02°. The standard uncertainty in H due to uncertainty in θ is 0.2 μm. The scale error of the laser has already been compensated for, and therefore, we do not consider any uncertainty in Hm itself. There is some linearity error in the probe's readings; we address that separately.

7.1.2. Uncertainty in the estimation of α. The standard uncertainty in the estimation of α is 0.078° as shown in section 4.5. Assuming that the nominal value of α is 1°, the standard uncertainty in H due to this term is negligibly small, less than 0.1 μm.

7.1.3. Uncertainty in the estimation of the vertical offset between probes. This does not impact height measurements as each probe makes an independent measurement of the height. The vertical offset only serves to tie the data from both probes into a common vertical scale.

7.1.4. Probe linearity. As mentioned in section 3, the probe readings have a ±5 μm linearity error. Over a 1 mm range of measurement, we assume that the probe has a ±2 μm linearity error (for both the top and bottom surfaces). Assuming that any value within this bound is equally probable (a uniform distribution), the standard uncertainty in H is $(2/\sqrt{3})\cos(25)\sqrt{2} = 1.5$ μm.

7.1.5. Probe repeatability. The repeatability error of the probe is within a ±2 μm bound and this error is along the probe's measurement direction (nominally at 25° with the Z axis). Its component along the Z axis will potentially contribute to an uncertainty in the detection of the height. We however average numerous data points, and therefore, the uncertainty in height is less than 0.1 μm.

7.1.6. Z straightness of the stage. The specification for the Z straightness of the Aerotech ALS 50060 stage is ±3 μm. Straightness does not vary rapidly over a short travel distance (say less than 10 mm travel). Assuming therefore that half the straightness forms upper bounds within which any value is equally likely, the standard uncertainty in height due to this term is 0.9 μm.

7.1.7. Part surface texture and form errors. While the surfaces of the graphite fuel cell plate might have local variations within a ±1 μm range, we average about 200 data points (covering 0.6 mm) at the top surface of the plate and 200 data points at the bottom surface of the channel to estimate the height. The uncertainty in the height reduces to less than 0.1 μm because of this averaging.

7.1.8. Repeatability from parallel profiles on the part. We measure parallel profiles on the fuel cell plate and average the height from the three traces. This is done to sample variations in height along the channel. The experimentally determined repeatability of 0.5 μm (one standard deviation) may possibly already sample some of the other terms described here, but we include it nevertheless.

7.1.9. Non-zero α and Y displacement. We show in figure 3 that if the misalignment angle α is non-zero, then the probe does not measure along the same Y position at all heights, i.e. while B is the intended probing location, the probe in fact measures point C in figure 3. This would pose a problem if the plate had some rotation about the X axis in which case the height measured by the probe would be larger or smaller than the true value. Assuming a bound of 1° for the misalignment angle α and a bound of 1° for the rotation about the X axis (assuming uniform distribution), we estimate an uncertainty of 0.4 μm in height.

Table 4. Uncertainty budget for height and width measurements on graphite fuel cell plates with nominally vertical side walls.

Source	Uncertainty in height (μm)	Uncertainty in width (μm)
System parameters		
Uncertainty in the estimation of the tilt angle θ	0.2	0.5
Uncertainty in the estimation of α	0.1	0
Uncertainty in the estimation of the vertical offset between probes	0	
Probe		
Probe linearity	1.5	1.4
Probe repeatability	0.1	0.1
Stage		
Z straightness of the stage	0.9	
Pitch motion of the stage		1.0
Uncertainty in encoder readings		0.1
Part		
Part surface texture and form	0.1	0.1
Repeatability from parallel profiles on part	0.5	1
Alignment		
Non-zero α and the Y displacement	0.4	
Part misalignment		0.1
Offset between probes along the Y axis		0.5
Other		
Realizing the definition of the measurand	0.2	0.2
Uncertainty in the estimation of the horizontal offset between probes		
(root sum square of above-described terms)		2.1
Combined standard uncertainty ($k = 1$)	1.9	3

7.1.10. Realizing the definition of the measurand. We defined the measurand (as realized by the UMAP system) in section 6. For the non-contact probe measurement, we did not employ a vacuum chuck and therefore the height was calculated as the distance between the bottom of a channel and the two neighboring land areas on the top surface (local height). We experimentally estimate the difference between our calculation and the measurand to introduce an uncertainty of 0.2 μm in height.

Combining the terms given above, we have a standard uncertainty in height measurement of 1.9 μm, or an expanded uncertainty of 3.8 μm ($k = 2$).

7.2. Width measurements

7.2.1. Uncertainty in the estimation of the tilt angle θ. Any uncertainty in the misalignment angle θ will result in an incorrect transformation of the raw data from the measured non-orthogonal to the corrected orthogonal frame. The result of an incorrect transformation is the introduction of an apparent taper in the side wall of the channel. But it should be noted that this taper occurs about the probe's zero reading; that is, the X coordinate of the point where the probe reads zero suffers no error. The X coordinates of points farther away from the probe's zero reading suffer greater errors. Therefore, the possibility for large width errors occurs if the channel is measured away from the center of the probe's range.

Assuming that a channel is 1 mm deep and further assuming that the probe was positioned so that the bottom surface of the channel is at the center of the probe's range, a conservative estimate for the standard uncertainty in the width (at the 1 mm position) due to a standard uncertainty of 0.02° in

θ is 0.5 μm. This value however changes to 2.5 μm when the part is positioned 5 mm away from the center of the probe's range. It is therefore important to position the part so that it is at the center of the probe's range. We assume 0.5 μm to be the standard uncertainty in width due to uncertainty in θ.

7.2.2. Uncertainty in the estimation of α. As shown in section 2, the misalignment angle α does not impact width measurements.

7.2.3. Probe linearity. As mentioned in section 3, the probes have a large linearity error of ±7 μm when measuring vertical surfaces such as the channel side wall. Over a short range of a couple of millimeters, we assume that the probe's linearity error is within a bound of ±4 μm where any value within this bound is equally likely. The component of this error acts along the X axis to produce an offset of the edge position. Combining the effects on both side walls, we obtain an uncertainty in the width of $(4/\sqrt{3}) \sin(25)\sqrt{2} = 1.4$ μm.

7.2.4. Probe repeatability. This term is similar to that described for height measurements, but the component along the X axis will now be of importance instead of the component along the Z axis. We average numerous data points, and therefore, the uncertainty in width is less than 0.1 μm.

7.2.5. Pitch motion of the stage. The pitch motion of the stage produces two effects—first, it produces an apparent taper in the side wall of the channel, and second, it produces an offset in the side wall position. The manufacturer's specification for the pitch is 17 arc-seconds. As in the case of straightness,

pitch also does not change by large amounts over short travel distances, such as the less than 1 mm width of a channel. Assuming that the pitch changes by only 5 arc-seconds (which we assume to be a bound for a uniform distribution) over 1 mm travel, the apparent taper in the side wall is 5 arc-seconds; this has a negligible effect on the width regardless of where the part is in the probe's range. The more noticeable effect is the offset produced in the side wall position because the part may be about 50 mm away from the top of the table. At this height, the standard uncertainty in the side wall location due to the pitch error is 0.7 μm. Combining this term with a similar effect on the other side wall, the uncertainty in the width due to pitch motion is 1 μm.

7.2.6. Uncertainty in encoder readings. The X axis encoder has a specification of ± 1 μm. The side wall position is determined from an average of numerous data points collected over the vertical face of the channel, and therefore, the uncertainty in the side wall position reduces to less than 0.1 μm (assuming that 500 data points are collected). The uncertainty in the width (determined from two side walls) is therefore 0.1 μm. It should be noted that averaging does improve the uncertainty in this case because the data points acquired on the side wall are all at different X positions as the geometry of the measurement in figure 3 shows.

7.2.7. Part surface texture and form. Side wall roughness and form will produce an uncertainty in the side wall position and therefore the width. Experiments with the UMAP system have shown that the side wall roughness is less than ± 2 μm and with significant averaging, the uncertainty in the side wall position and the width reduces to less than 0.1 μm.

7.2.8. Repeatability from parallel profiles on the part. We experimentally determine a repeatability of 1 μm (see section 7.1 for description).

7.2.9. Part misalignment. Any rotations of the part about the Z axis will cause the measured width to be larger than the true width (i.e. the channels are not aligned along the Y axis but rotated by a small amount). Assuming that any misalignment within a bound of $\pm 1°$ is equally likely, for a channel 1 mm wide, the standard uncertainty in width is less than 0.1 μm. There is also another effect associated with this misalignment. In presence of a non-zero probe misalignment angle α (assumed to be 1°) in conjunction with part misalignment considered here, there is an additional uncertainty of 0.1 μm. This uncertainty source can be explained using figure 3. As the probe travels the vertical wall, and if the part is perfectly aligned, the probe moves from point O to point C on one side wall. If the part is not aligned, point C is displaced along the X axis by some extent. The same situation occurs on the other side. Depending on the misalignment angle α of the second probe, the errors in the estimation of the side wall positions may sum or cancel each other.

7.2.10. Offset between probes along the Y axis. The two probes are aligned along the Y axis to within 0.05 mm. If the channels are not aligned along the Y axis, any offset between the probes will cause the channel width to either appear larger or smaller depending on the geometry of the measurement. Assuming a bound of 1° for this misalignment, we estimate an uncertainty in width of 0.5 μm from this source.

7.2.11. Realizing the definition of the measurand. We defined the measurand in section 6. Two-point width measurements using the non-contact probe will be extremely noisy, and we therefore estimated the width as the average over a 0.2 mm region along the side wall of the channel. We experimentally estimate an uncertainty of 0.2 μm from this discrepancy in realizing the definition of the measurand.

7.2.12. Uncertainty in the estimation of the horizontal offset between probes. The above-described terms are combined to produce a standard uncertainty of 2.1 μm in the determination of the width of a channel. However, the measured width has to be corrected by the probe offset w. This probe offset is also determined from a width measurement, but performed on an artifact of known width; it therefore also has an uncertainty of 2.1 μm. The uncertainty in the width of the calibrated artifact is itself negligibly small in comparison.

The combined standard uncertainty in the channel width is therefore 3 μm. The expanded uncertainty is 6 μm ($k = 2$).

8. Summary

In this paper, we describe a system for performing rapid, yet accurate, dimensional measurements on bipolar fuel cell plates using laser triangulation probes. In order to obtain side wall information, we employ two probes that are tilted in opposing directions. The use of two tilted probes necessitates the determination of six system parameters using a calibration procedure which we have detailed.

A primary contributor to the uncertainty in our measurements is the linearity error in the triangulation probe. This affects both height and width measurements. Of the six system parameters, the tilt angle θ is perhaps the most important. It influences both height and width measurements, although its impact is not as severe as the probe's linearity errors. Any error in the tilt angle will result in an apparent taper in the side wall of the channel and therefore contribute an uncertainty to any feature of interest pertaining to the side wall, such as side wall taper and width.

We measured numerous bipolar fuel cell plates using our system and compared our measurements with the results obtained using a UMAP system. Our measurement and analysis show width and height errors of less than ± 1 μm on calibrated gauge blocks and less than ± 2 μm on channel width and height of fuel cell plates. We estimate an expanded uncertainty of 6 μm ($k = 2$) on channel width and 3.8 μm ($k = 2$) on channel height for graphite bipolar fuel cell plates with vertical side walls.

Acknowledgments

References

[1] Tawfik H, Hunga Y and Mahajan D 2007 Metal bipolar plates for PEM fuel cell—a review *J. Power Sources* **163** 755–67

[2] Hermann A, Chaudhuri T and Spagnol P 2005 Bipolar plates for PEM fuel cells: a review *Int. J. Hydrogen Energy* **30** 1297–302

[3] Stanfield E 2008 Metrology for fuel cell manufacturing *Annual Progress Report* Department of Energy http://www.hydrogen.energy.gov/pdfs/progress08/vi_3_stanfield.pdf

[4] Wheeler D and Sverdrup G 2008 2007 Status of manufacturing: polymer electrolyte membrane (PEM) fuel cells *Technical Report* NREL/TP-560-41655 National Renewable Energy Laboratory (NREL)

[5] Liu D, Peng L and Lai X 2009 Effect of dimensional error of metallic bipolar plate on the GDL pressure distribution in the PEM fuel cell *Int. J. Hydrogen Energy* **34** 990–7

[6] Mahabunphachai S, Cora Ö N and Koc M 2010 Effect of manufacturing processes on formability and surface topography of proton exchange membrane fuel cell metallic bipolar plates *J. Power Sources* **195** 5269–77

[7] Weckenmann A, Peggs G and Hoffmann J 2006 Probing systems for dimensional micro- and nano-metrology *Meas. Sci. Technol.* **17** 504–9

[8] Weckenmann A, Estler T, Peggs G and McMurtry D 2004 Probing systems in dimensional metrology *CIRP Ann.* **53** 657–84

[9] Garces A, Huser-Teuchert D, Pfeifer T, Scharsich P, Torres-Leza F and Trapet E 1993 Performance test procedures for optical coordinate measuring probes *Final Project Report: part 1* European Communities, Brussels, contract no 3319/1/0/159/89/8-BGR-D (30)

[10] Laser Measurement Product Brochure, *Keyence LK-G series product catalog* http://www.keyence.com/products/measure/measure/laser/lkg/lkg.php